

Spectral Width of Optically Generated Bottlenecked 29-cm^{-1} Phonons in Ruby

J. I. Dijkhuis, A. van der Pol, and H. W. de Wijn
Fysisch Laboratorium, Rijksuniversiteit, Utrecht, The Netherlands
 (Received 24 August 1976)

The ruby R_2 -line intensity at 2.1 K is observed to be nearly quadratically dependent on the R_1 intensity, indicative of strongly bottlenecked 29-cm^{-1} phonons generated by the $2\bar{A}(^2E) \rightarrow \bar{E}(^2E)$ decay in the optical pumping cycle. The spectral width of the phonon excitation is probed by separating the degenerate phonon packets in a magnetic field and monitoring the decrease of the bottlenecking.

Bottlenecking of acoustic phonons resonant between the optically excited metastable $\bar{E}(^2E)$ state of Cr^{3+} in ruby and the $2\bar{A}(^2E)$ state 29 cm^{-1} higher has been observed at liquid helium temperatures during recent years. The first demonstration¹ of the reality of bottlenecked 29-cm^{-1} phonons was through the slowing down, with increasing excited-state population, of the Orbach relaxation² between the \bar{E} magnetic substates via $2\bar{A}$ as intermediate level. Subsequently, local imprisonment of 29-cm^{-1} phonons produced with heat pulses was shown to exist by monitoring intensity changes of the R_2 luminescent line.³ In this Letter, we report first on a new and different method of generating bottlenecked 29-cm^{-1} phonons in ruby, viz., by the nonradiative decay of the optical pumping cycle in the temperature regime where thermalization is essentially absent ($T < 3$ K). Secondly, we present a scheme of probing the spectral width of the bottlenecked phonon excitation by separating the Zeeman components of the transition in a magnetic field.

Under the condition of stationary optical pumping, the optical feeding into the metastable levels equals the radiative decay to the ground state. Below 3 K, where the R_2 luminescence is weaker than the R_1 luminescence by many orders of magnitude, the R_1 intensity therefore is, apart from a measure of the excited-state population, a direct gauge for the feeding into $2\bar{A}$. On the other hand, the $2\bar{A}$ population, which is accessible to measurement through the intensity of the R_2 luminescence, decays predominantly to the \bar{E} state. Balancing the feeding and the decay, and noting that the transition probabilities of the R_1 and R_2 lines are about the same, we have for the effective decay time between $2\bar{A}$ and \bar{E}

$$T_{2\bar{A} \rightarrow \bar{E}}^{\text{eff}} / \tau_R \approx R_2 / R_1, \quad (1)$$

where $\tau_R \approx 4$ ms is the radiative lifetime of the R_1 line, while R_1 and R_2 henceforth denote the integrated luminescent intensities. Under bottlenecking conditions the reabsorption $\bar{E} \rightarrow 2\bar{A}$ of reso-

nant 29-cm^{-1} phonons becomes a process with a rate competing with the spontaneous decay $2\bar{A} \rightarrow \bar{E}$. As a result the net decay rate $1/T_{2\bar{A} \rightarrow \bar{E}}^{\text{eff}}$ will be slowed down relative to the spontaneous rate $1/T_{2\bar{A} \rightarrow \bar{E}}$, and R_2 will no longer be proportional to R_1 .

The excited-state population is maintained by continuous pumping with a 1-W argon laser tuned to 514.5 nm. At the highest intensities the focused laser beam is capable of exciting a good fraction of the ground state population in the $\sim 700\text{-ppm}$ ruby crystal, which was immersed in liquid helium below the λ point. A double monochromator was employed to suppress the instrumental wings of the R_1 line at the position of the much weaker R_2 line. A cooled photomultiplier and photon counting assured sensitivity and linearity of the detection system. Neutral density filters were used to avoid overload.

The experimental dependence of R_2 on R_1 at 2.1 K is shown in Fig. 1. It is observed that the dependence of R_2 on R_1 is close to quadratic (exponent 2.1 ± 0.1). In other words, the population dependence of $T_{2\bar{A} \rightarrow \bar{E}}^{\text{eff}}$ is close to linear, indicative of a situation of complete bottlenecking throughout the region of intensities shown.⁴ It is noted here that lowering the temperature to 1.5 K does not affect these results, ruling out residual heating of the crystal by the pumping light. One may estimate $T_{2\bar{A} \rightarrow \bar{E}}^{\text{eff}}$ and the bottlenecking factor $\sigma = T_{2\bar{A} \rightarrow \bar{E}}^{\text{eff}} / T_{2\bar{A} \rightarrow \bar{E}}$ associated with it from Eq. (1). At the highest intensity $T_{2\bar{A} \rightarrow \bar{E}}^{\text{eff}} \approx 0.002 \tau_R \approx 10 \mu\text{s}$ and, with $T_{2\bar{A} \rightarrow \bar{E}} \approx 10^{-9}$ s,^{3,5} $\sigma \approx 10^4$. Similarly, at the lowest intensities in Fig. 1, $T_{2\bar{A} \rightarrow \bar{E}}^{\text{eff}} \approx 0.2 \mu\text{s}$ and $\sigma \approx 200$.

The spectral width of the "hot" optically generated 29-cm^{-1} phonons, a principal point of interest in this Letter, is accessible to experiment by observing the change of R_2 upon applying a magnetic field. The $2\bar{A} \rightarrow \bar{E}$ line is gradually split by the Zeeman effect into four distinct transitions. With the same optical feeding into $2\bar{A}$, the number of phonon modes to be bottlenecked there-

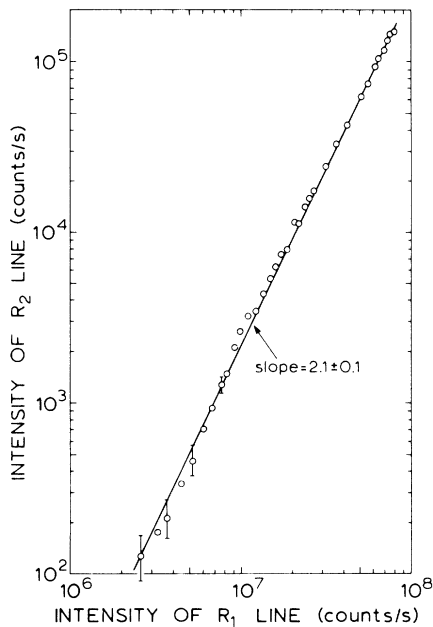


FIG. 1. The integrated intensity of the R_2 line vs the integrated intensity of the R_1 line at 2.1 K for a 700-ppm ruby sample. The slope of 2.1 ± 0.1 indicates strong bottlenecking ($\sigma \sim 10^2 - 10^4$) of optically generated 29 cm^{-1} phonons.

by increases relative to the zero-field case until ultimately each of the four Zeeman components is exclusively on speaking terms with its own phonon packet. The degree of bottlenecking will thus decrease with field, resulting in a reduction of the $2\bar{A}$ population maintained in the bottleneck and the corresponding R_2 intensity. The precise field dependence of R_2 of course depends on the g factors of $2\bar{A}$ and \bar{E} , and the shape and further characteristics of the phonon packets, but roughly speaking the width of the bottlenecked phonons manifests itself in the form of the "width" of the field dependence.

Experimental data on the field dependence of R_2 at constant optical feeding are collected in Fig. 2 for several excited-state populations in the bottlenecked regime. At the highest excited-state population ($N \sim 10^{19}/\text{cm}^3$) substantial separation of the phonon packets is already attained at 500 G, while full separation is reached beyond 1.5 kG, where R_2 levels off at about $\frac{1}{4}$ of the zero-field intensity. At lower excited-state population the packet width appears to be effectively smaller. In the inset to Fig. 2 the width of the field dependence δH is shown to saturate finally at the higher populations.

The transition $2\bar{A} \rightarrow \bar{E}$ may be thought of as having a line shape inhomogeneously broadened by,

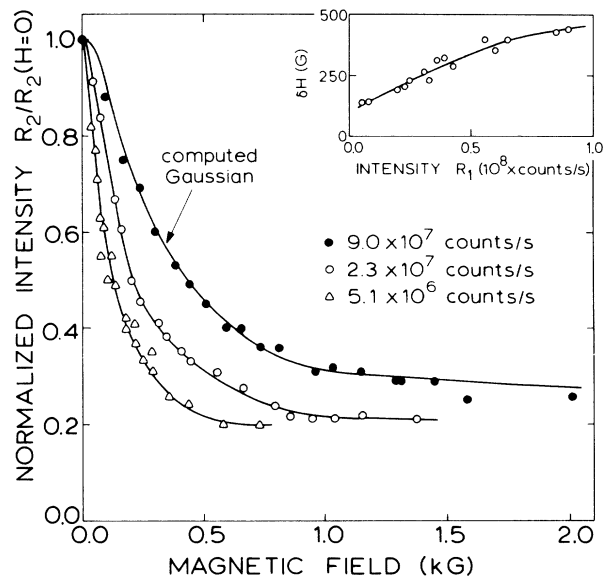


FIG. 2. The integrated intensity of the R_2 line, normalized to zero field, vs the magnetic field parallel to the c axis at 2.1 K for several excited-state populations as measured by the R_1 intensity. The curve through the data points with $R_1 = 9.0 \times 10^7$ counts/s has been computed for a homogeneous Gaussian resonance line with half-value width 0.017 cm^{-1} , as explained in text. The inset gives the field δH at which $R_2/R_2(H=0) = 0.5$ vs R_1 .

e.g., local strains in the crystal. The half-value width is $\sim 0.02 \text{ cm}^{-1}$, as will appear below, an order of magnitude larger than the spontaneous decay width $1/2\pi T_{2\bar{A} \rightarrow \bar{E}} \approx 0.002 \text{ cm}^{-1}$. The region of bottlenecking then extends to a point in the wings, dependent on the \bar{E} population, where the number of interruptions of a phonon within its lifetime has become unity, while the spectral distribution of the phonons has the same form as the $2\bar{A} \rightarrow \bar{E}$ transition. However, under strong bottlenecking conditions ($\sigma \gg 1$) the line will be homogenized to some extent by spectral redistribution of the phonons. The change of the phonon frequency per absorption of a phonon in a spin-flip transition $\bar{E} \rightarrow 2\bar{A}$, followed by the emission of a phonon in a spin-nonflip transition $2\bar{A} \rightarrow \bar{E}$, or vice versa, is of the order of the dipole-dipole splitting of the \bar{E} level, which is about 0.002 cm^{-1} at our ground-state concentration, irrespective of any further spin-dependent inhomogeneous broadening of the \bar{E} substates.⁶ The range of this random-walk spectral redistribution, expected to scale with the square root of the number of interruptions of a phonon within its lifetime, or roughly $\sigma^{1/2}$, is largest in the center of the bottlenecked line and gradually becomes

smaller towards the wings. As a result the spectral distribution of the phonons is smeared out about the line center. With increasing population of the \bar{E} state the interruption rate of a phonon increases, and the area of spectral redistribution broadens correspondingly, until under extreme bottlenecking conditions the line becomes spectrally diffusive over a region many times broader than its width. The phonon distribution has then leveled off over a diffusive region which virtually coincides with the entire bottlenecked area.

At lower bottlenecking, the experiments in Fig. 2 suggest a limited area of spectral redistribution in the central area of the inhomogeneous line. Applying a magnetic field provides an additional mechanism, similar to dipolar homogenization, that brings the homogenized central area in contact with the wings, viz., spin-flip absorption $\bar{E} - 2\bar{A}$ followed by spin-nonflip emission $2\bar{A} - \bar{E}$ of a phonon, or vice versa, changing the phonon frequency by the Zeeman splitting. Apart from the decrease of the bottlenecking induced by the gradual Zeeman splitting into four distinct phonon packets, the resultant migration of the phonon excitation to the wings further reduces the bottlenecking as soon as the Zeeman splitting exceeds the dipolar splitting. The effects are of course smaller the farther the spectrally diffusive region extends into the wings, until for a line already fully homogenized at zero field the effects are completely masked. In Fig. 2 it is indeed observed that the drop of R_2 with field is steeper, the lower the bottlenecking. The case with $R_1 = 9.0 \times 10^7$ counts/s, for which δH is approaching saturation, is apparently close to full homogenization.

The rate equations governing the occupation of the sublevels of the \bar{E} and $2\bar{A}$ states and the phonon occupation numbers are numerically solved for various resonance line shapes with neglect of thermal phonons and in the stationary case. To make the model mathematically tractable, instantaneous spectral redistribution, which occurs in the limiting case of infinite bottlenecking, is assumed between the phonons within the bottlenecked region of the $2\bar{A} - \bar{E}$ resonance line, and further it is assumed that the phonons decay with a lifetime³ $T_{LB} \sim 10^{-6}$ s to "sinks" uniformly distributed throughout the crystal.⁷ A similar model, but for a two-level scheme corresponding to the zero-field situation in our case, is used by Giordmaine and Nash,⁴ who calculated the relaxation time in the bottlenecked regime for several

line shapes as a function of the concentration of bottlenecking centers. In agreement with their results, we find in the zero-field case an increase of the $2\bar{A}$ population with the 3/2 and second power of the total metastable occupation for Lorentzian and Gaussian line shapes, respectively. These results only apply to the upper part of Fig. 1, where the bottlenecking is sufficiently strong to have substantial homogenization.⁸ It is concluded that the experimentally found power of 2.1 ± 0.1 is in accord with a Gaussian-type line shape rather than a Lorentzian one.

The magnetic field dependence of the $2\bar{A}$ population with constant pumping under very strong bottlenecking conditions ($\sigma \sim 10^4$), calculated with the four-level model discussed above, is inserted in Fig. 2 in the case of $R_1 = 9.0 \times 10^7$ counts/s for a Gaussian resonance line with a half-value width of 0.017 cm^{-1} ,⁹ i.e., with a width fitting the experimental decrease of R_2 . For the case in point, the width of the homogenization of the bottlenecked phonon packet then is $\sim 0.017(\ln\sigma)^{1/2} = 0.05 \text{ cm}^{-1}$, so that the assumption of a fully homogenized line and diffusion to transparent wings is indeed found to apply.¹⁰ It is noteworthy here that, under the same conditions, in case of a homogeneous Lorentzian line with a width as small as the spontaneous decay ($\approx 0.002 \text{ cm}^{-1}$), magnetic fields of ~ 4 kG would be required to reduce R_2 by 50%, in contrast to experiment and corroborating the above conclusion that the line is of Gaussian type.

In summary, it is concluded that a Gaussian-type resonance line with half-value width 0.02 cm^{-1} , homogeneous through strong spectral redistribution of the phonons, provides an excellent description of both the close to quadratic dependence of R_2 on R_1 and the experimental decrease of R_2 with field at high bottlenecking. However, at lower bottlenecking spectral diffusion appears to be confined to the central part of the transition.

We are grateful to G. J. Dirksen for crystal growing.

¹R. Adde, S. Geschwind, and L. R. Walker, in *Magnetic Resonance and Radio frequency Spectroscopy: Proceedings, Colloque Ampère IV*, edited by P. Averbuch (North-Holland, Amsterdam, 1969), p. 460.

²S. Geschwind, G. E. Devlin, R. L. Cohen, and S. R. Chinn, *Phys. Rev.* **137**, A1087 (1965).

³K. F. Renk and J. Deisenhofer, *Phys. Rev. Lett.* **26**, 764 (1971); K. F. Renk and J. Peckenzell, *J. Phys.* (Paris), *Colloq.* **4**, 103 (1972).

⁴J. A. Giordmaine and F. R. Nash, Phys. Rev. **138**, A1510 (1965).

⁵N. A. Kurnit, I. D. Abella, and S. R. Hartman, in *The Physics of Quantum Electronics Conference Proceedings, San Juan, Puerto Rico, 1965*, edited by P. L. Kelley, B. Lax, and P. E. Tannenwald (McGraw-Hill, New York, 1966), p. 267.

⁶This mechanism in a *static* dipolar field is absent in a two-level system, where homogenization must occur during the time spent in the upper level. Lifetime broadening of $2\bar{A}$ cannot homogenize the phonon frequencies. See P. W. Anderson, Phys. Rev. **114**, 1002 (1959).

⁷P. G. Klemens, J. Appl. Phys. **38**, 4573 (1967).

⁸The change in effective width of the phonons with the metastable population (inset to Fig. 2) would slightly reduce the calculated power. However, this could easily

be offset by residual effects of spatial diffusion, which predicts a third power (Ref. 4).

⁹This is one order of magnitude smaller than the observed width of the *R* lines. The calculated ratio of the *R* lines. The calculated ratio of the broadening due to random crystal fields between $2\bar{A} \leftrightarrow \bar{E}$ and the *R* lines is ~ 0.1 (V. M. Hol and H. W. de Wijn, unpublished calculations), in agreement with our findings.

¹⁰At the highest excited-state populations reached in our experiments the interruption rate of a phonon $\sigma/T_{LB} \approx 10^4/10^{-6} = 10^{10}$ Hz is comparable with the resonance linewidth of 0.02 cm^{-1} , so that the reactive coupling (Ref. 4) between the phonons and the spins is beginning to play a part. In our case the effects are small, but in more concentrated ruby the coupling may be observable.

Cationic Short-Range Order in the Hollandite $\text{K}_{1.54}\text{Mg}_{0.77}\text{Ti}_{7.23}\text{O}_{16}$: Evidence for the Importance of Ion-Ion Interactions in Superionic Conductors

H. U. Beyeler

Brown Boveri Research Centre, CH-5401 Baden, Switzerland

(Received 13 July 1976)

Analysis of the diffuse x-ray scattering in the one-dimensional ionic conductor $\text{K}_{1.54}\text{Mg}_{0.77}\text{Ti}_{7.23}\text{O}_{16}$ (hollandite) yields a detailed microscopic picture of the cationic short-range order. This order is characterized by large shifts of some ions off their crystallographic sites, evidencing that in a superionic conductor the ion-ion interaction may be stronger than the periodic potential of the host crystal.

The rapidly growing interest in electrochemical devices based on solid electrolytes has stimulated an intensive search for new materials with high ionic conductivities, the so-called superionic conductors.¹²

The mobile ions in a superionic conductor typically reside on a fractionally occupied sublattice with open pathways between adjacent sites. The number of sites available to the mobile ions is often not much larger than the number of occupied sites, and diffusion in such systems is no longer a single-particle process as described by the traditional random-walk theory. The path probability method by Sato and Kikuchi³ is a major and significant step towards a correct description of diffusion in concentrated systems. More recently, Monte Carlo calculations have been performed on simple model systems⁴ which go beyond the nearest-neighbor interaction of the path probability method.

Experimental and theoretical studies of the dynamics of ionic motion in superionic conductors⁵ have shown that interaction among the mobile ions leads to structure in $\sigma(\omega)$ in the frequency range of a typical jump rate and affects the parameters describing the high-frequency behavior. The

structure of the static short-range order among the mobile species gives in principle the most direct information about ion-ion interactions; but, unfortunately, the complex diffuse x-ray scattering observed in solid electrolytes⁶⁻⁸ inhibits in general an unambiguous determination of the local atomic arrangement.

By considering a one-dimensional model system with the hollandite structure, I have now for the first time been able to obtain a precise microscopic picture of the state of order in a solid electrolyte. My results give direct evidence that the effective ion-ion interaction in a solid electrolyte is potentially of the same strength as the periodic potential of the host crystal. As a consequence, all models which treat ion-ion interactions in terms of occupational short-range order are incomplete, and it is necessary to include strong deviations of the equilibrium positions from crystallographic sites.

In the composition $\text{K}_{2x}\text{Mg}_x\text{Ti}_{8-x}\text{O}_{16}$ ($0.75 \leq x \leq 1$), hollandite^{9,10} consists of a framework of edge- and corner-sharing TiO_6 and MgO_6 octahedra forming parallel, nonintercommunicating channels of nearly square cross sections along the *c* axis of the tetragonal unit cell. The distance be-